Effect of a Dwell Stage in the Cure Cycle on the Interphase Formation in a Poly(ether imide)/High T_g Epoxy System

Farooq, Ujala; Heuer, Sönke; Teuwen, Julie; Dransfeld, Clemens

DOI
10.1021/acsapm.1c00956

Publication date
2021

Document Version
Final published version

Published in
ACS Applied Polymer Materials

ACS APPLIED POLYMER MATERIALS

pubs.acs.org/acsapm

Article

Effect of a Dwell Stage in the Cure Cycle on the Interphase Formation in a Poly(ether imide)/High T_g Epoxy System

Ujala Farooq,* Sönke Heuer, Julie Teuwen, and Clemens Dransfeld

Cite This: https://doi.org/10.1021/acsapm.1c00956

Read Online

ACCESS | Metrics & More | Article Recommendations | Supporting Information

ABSTRACT: Epoxies are inherently brittle materials and to overcome this brittleness, a second microphase (i.e., thermoplastic) is typically added. This modification of epoxy resin using thermoplastics results in reaction-induced phase separating morphologies in the micrometer range. In this study, the influence of the curing history, beyond phase separation, on the interphase formation and final morphology of PEI and the high T_g epoxy system is investigated. Several cure cycles were examined, each with a first dwell temperature ranging from 120 to 180 °C for a given time up to the onset of phase separation (OPS) or up to the 80% degree of cure (80% DOC) and then with a second dwell at 200 °C for 20 min to complete the cure cycle. Hot-stage microscopy experiments were carried out at several first dwell temperatures before final conversion at the second dwell. The morphologies and resulting droplet size distribution at the interphase, after the final cure, were analyzed through scanning electron microscopy. Results showed that the diffusion distance was significantly higher in the case of OPS as compared to the 80% DOC case, particularly at lower first dwell temperatures. This behavior was attributed to the fact that, in the case of OPS, polymeric chains were still in a mobile state and diffused further during the second dwell curing stage, while at 80% DOC, polymeric chains were completely bound but still diffuse due to non-stoichiometric curing. This restricted mobility of polymeric chains after phase separation (80% DOC) resulted in a larger number of smaller droplets as compared to the OPS case.

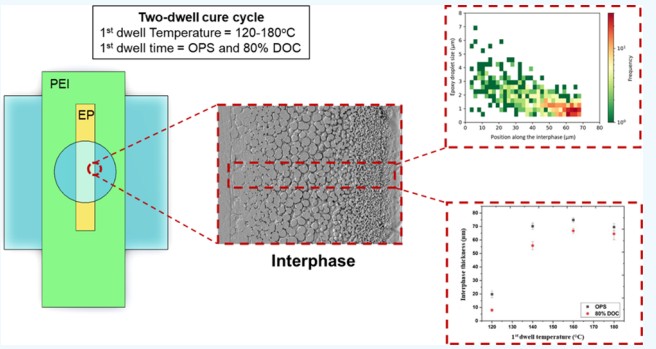

KEYWORDS: *epoxy, poly(ether imide) (PEI), interphase formation, morphology, curing cycle, reaction induced phase separation, diffusion*

1. INTRODUCTION

Thermosetting epoxy systems are commonly used as a matrix component of carbon fiber-reinforced polymers (CFRPs) due to their high mechanical properties and ease of processing.[1] However, epoxies display inherently brittle behavior with poor crack resistance and low fracture toughness at room temperature.[2,3] To overcome these drawbacks, strategies have been developed to successfully enhance the fracture toughness of epoxies.[4,5] A strategy to toughen the epoxy resins is the addition of a second microphase (i.e., thermoplastic, rubber, nanofiller, block copolymer, etc.) into the epoxy system,[6−9] some of which result in morphologies through reaction-induced phase separation.[10] Poly(ether imide) (PEI) has been reported as a potential modifier for epoxy resins particularly for aerospace applications due to the high glass transition temperature (217 °C), good miscibility due to its amorphous state, and compatibility with epoxy systems, enhanced rigidity, and strength at higher temperatures.[11]

To toughen the brittle epoxy, the thermoplastic microphase is incorporated into the epoxy system followed by the curing reaction. Curing, or the cross-linking reaction, of epoxy is frequently done by performing either one or two dwell cycles (Figure S1, see the Supporting Information). The two-dwell cycle approach is preferably used because it facilitates the processing of epoxy and allows the evacuation of voids before final curing.[12] During curing of epoxy-amine systems, three main reactions take place: (i) the epoxy group reacts with a primary amine to produce a secondary amine, (ii) the secondary amine further reacts with an epoxy group to create a tertiary amine, and (iii) at higher temperatures, unreacted epoxy groups also react with reacted epoxy to make an ether bridge.[13−15]

During the curing process, liquid reactive thermoset monomers (TS) diffuse into the glassy thermoplastic (TP) and partially swell or dissolve it, which results in the diffusion of thermoplastic polymeric chains (TP) into the resin (TS). This interdiffusion process tends to slow down and eventually

Received: August 3, 2021
Accepted: November 7, 2021

stops after reaching the gel point due to the constrained mobility of the thermoset.[16] The mutual diffusion of the components (TS and TP) into each other creates a concentration gradient in the interfacial region. At the onset, this phenomenon can be described as solvents diffusing into glassy polymers.[17] The interfacial region, surrounded by the pure phases (epoxy and PEI), can be further identified in three different regions in the thermoplastic-epoxy diffusion zone, according to the amount of decreasing polymer concentration, i.e., (i) infiltration layer, (ii) swollen gel layer, and (iii) liquid layer. The liquid layer is a diluted polymer solution with relatively free motions of entire polymer chains. The gel layer is a swollen polymer in a rubber-like state. In the infiltration layer, Fickian diffusion of the solvent molecules is observed. The epoxy penetration front between the gel layer and the infiltration layer is sharp and advances at a constant rate. This is usually referred to as case II diffusion.[17] The proceeding reaction between the thermosetting co-monomers eventually results in a reaction-induced phase separation, leading to a gradient morphology in the interfacial zone,[17] where epoxy-rich droplets can be observed, reducing in size toward the pure thermoplastic (see Figure S2). The final morphology of the thermoset/high-T_g thermoplastic interphase results from the competition between the rate of phase separation and the simultaneous cross-linking.[18,19] In addition to this, the final morphology that formed between a thermoset and a thermoplastic is controlled by the molecular structure of the thermoplastic (i.e., degree of functionality and end-group chemistry), thermoplastic content, molecular weight of the thermoplastic, dwell temperature, solubility parameters of the components, dwell time, stoichiometric ratio of curing agent to epoxies, curing agent chemistry and functionality, presence and type of accelerator, and molecular structure of epoxy resins.[20]

The phase behavior is primarily controlled by the Cahn−Hilliard free energy with solution limited dynamics, which evolves during curing. Two mechanisms govern the phase separation in epoxy resin toughened with thermoplastic, known as (i) nucleation and growth (N&G) and (ii) spinodal decomposition (SD). The nucleation and growth mechanism begins with the creation of nuclei, which develops with reaction time to form spherical-like micro- or macro-separated domains of a thermoplastic-rich phase in a thermosetting resin. However, in the case of spinodal decomposition, the micro- or macro-separated domains of the thermoplastic-rich phase are highly interconnected.[21] These resultant morphologies can be finely tuned by varying the thermoplastic concentration in the blend and/or by changing the cure conditions.[22] Also, a different phase behavior has been observed between epoxy monomers and different glassy polymers, i.e., PES having an upper critical solution temperature (UCST)[23] and PEI having a lower critical solution temperature (LCST).[11]

In the literature, the effect of curing parameters (i.e., dwell temperature and conversion, cure cycle, etc.) for one (isothermal) dwell cure cycle has been experimentally investigated on the interphase formation, final morphology, and fracture toughness of epoxy and thermoplastic systems. For instance, Harismendy et al.[22] reported the effect of different dwell temperatures (140, 160, and 180 °C) on the morphological behavior of the epoxy/PEI system. Higher fracture toughness was observed for the samples having bigger droplets of epoxy (i.e., phase inversion) that formed at higher dwell temperatures.[22,24] Likewise, an increase in droplet size with the increasing dwell temperature has been observed in the literature for an epoxy system toughened with PEI.[25] On the other hand, Bian et al.[26] described the effect of cure temperature and thermoplastic content on the interphase thickness and the resultant fracture toughness of the modified epoxy system. The experimental outcome showed a higher fracture toughness for samples cured at higher temperatures, which was attributed to a higher interphase thickness. In addition to dwell temperature, dwell conversion of epoxy resin (before adding thermoplastic phase) has also been reported to significantly influence the morphology spectrum of the epoxy/PEI system.[27] Previously, our research group investigated the effect of dwell temperatures on the diffusion process for a high T_g epoxy system with PEI, which showed an increase in diffusion length and interphase dimension between the thermoset and PEI with an increasing dwell temperature.[18]

Previously, it was assumed that the diffusion process stops with the occurrence of the phase separation for the single dwell cure cycle.[17,18,28,29] Recently, Voleppe et al.[30] reported that the penetration front of the thermoset seemed to continue beyond phase separation for the epoxy and polyethersulfone (LCST)-based system using one dwell cure cycle. However, the influence of the curing history beyond phase separation, using two dwell cure cycles with varying dwell times/degrees of cure, on the interphase dimension and final morphology for poly(ether imide) having a contrasting phase behavior (UCST), is not well understood.

The research work presented in this paper aims to understand the interphase formation to later attain the desired droplet size and interphase morphology for improved material toughness. This aim is achieved by analyzing the influence of dwell time by considering two main cases for each selected first dwell temperature (120−180 °C): (i) waiting until the onset of phase separation (OPS) before increasing the temperature to 200 °C (second dwell) and (ii) waiting until 80% degree of cure (80% DOC) before the second dwell. To that end, time-lapse hot-stage microscopy experiments were carried out at several first dwell temperatures in a range of 120−180 °C, leading to the onset of phase separation or 80% degree of cure before the final conversion at the second dwell. The interphase formation and relevant interphase dimensions were studied through these microscopy experiments, and observations were subsequently related to the degree of cure through the use of a cure kinetics model. The morphologies present at the interphase were analyzed through scanning electron microscopy on etched samples.

2. MATERIALS AND METHODS

2.1. Materials. Poly(ether imide) (PEI) (Ultem 1000, molecular weight = 55,000 g/mol, $n \approx 90$, T_g = 217 °C) was used as the thermoplastic in the form of thin films (60 μm) provided by SABIC, Saudi Arabia. A blend of M-(2,3-epoxypropoxy)-*N*,*N*-bis(2,3-epoxypropyl)aniline (TGMAP, Araldite MY 0610 CH) and bisphenol-F epoxy resin monomer (DGEBF, Araldite PY 306 CH) was used as the thermoset resin. 3,3′-Sulfonyldianiline (DDS, Aradur 9719-1) was used as a curing agent for epoxy. These chemicals were supplied by Huntsman, Switzerland. The epoxy system is characteristic for aerospace composites prepregs with a cure temperature of 180 °C.

2.2. Cure Cycle. In this study, the effect of first dwell time and temperature of two-dwell cure cycles is investigated to study their influence on the interphase formation and morphology. Therefore, the final curing step also referred to as the second dwell time and temperature (t_{cure} and T_{cure}, respectively) was kept constant for the epoxy/PEI system, while the first dwell time and temperature (t_{dwell}

https://doi.org/10.1021/acsapm.1c00956
ACS Appl. Polym. Mater. XXXX, XXX, XXX−XXX

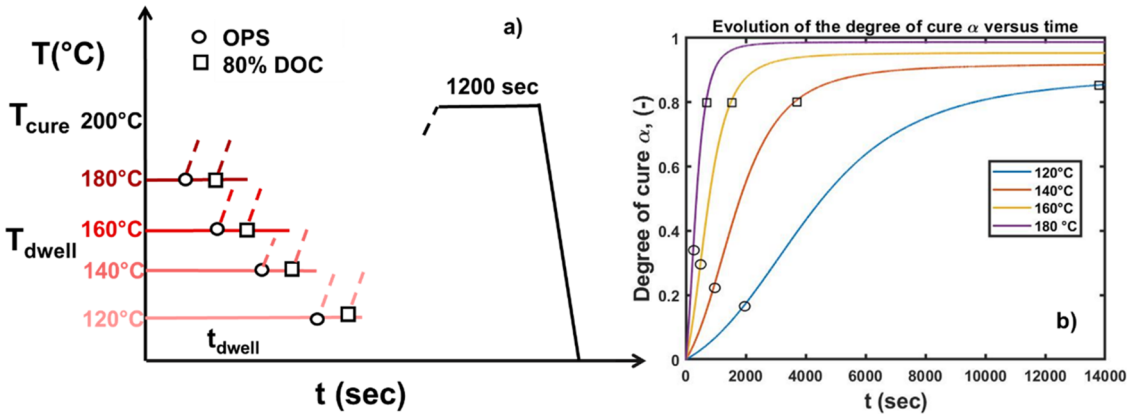

Figure 1. (a) Representative two-dwell cure cycle used for experiments with variable first dwell time and temperature. (b) Degree of cure and onset of phase separation at different cure temperatures for the epoxy/PEI system for a one-dwell cure cycle; circles represent the degree of cure at OPS, while squares represent 80% DOC.

and T_{dwell}, respectively) was varied in the study (Figure 1a). The selection of first and second dwell temperatures and times was based on the cure kinetics model of the epoxy system,[18] as shown in Figure 1b. It is evident that complete cure (degree of cure = 1) can be achieved at 180 °C or higher (Figure 1b). Therefore, a second dwell temperature of 200 °C along with a second dwell time of 20 min was used. Two different first dwell times (t_{dwell}) corresponding to (i) the onset of phase separation (OPS shown by circles in Figure 1b) and (ii) 80% degree of cure (80% DOC, shown by squares in Figure 1b) were selected for each investigated first dwell temperature. In our previous research, it was also shown that the interphase thickness varies as a function of cure temperature ranging from 120 to 180 °C (one dwell cure cycles).[16] Therefore, in this study, four different first dwell cure temperatures of 120, 140, 160, and 180 °C were selected (Table S1). All the samples were prepared and analyzed in triplicate.

2.3. Hot-Stage Experiments. Hot-stage microscopic analysis was performed to observe the epoxy/PEI interphase formation under different conditions. Figure 2 shows the schematics of the

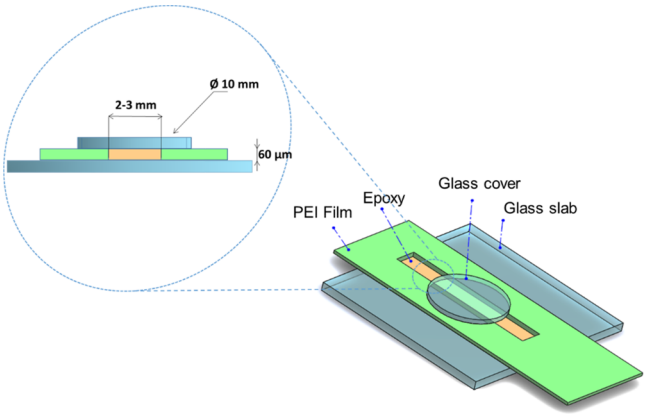

Figure 2. Schematic representation of the sample used for hot-stage microscopic analysis.

experimental setup used for hot-stage analysis. A PEI film with a thickness of 60 μm, having a 2−3 mm-wide central slit, was carefully sandwiched between two cover glasses. The PEI sandwich structure was placed on a temperature-controlled microscope stage THMS600 (Linkam Scientific, UK). The selected cure cycle was programmed in the Linkam software. The reactive liquid epoxy, at room temperature, was then injected into the slit region of the PEI film. The resin drop spontaneously attained the specimen temperature by having contact with the hot stage and filled the gap by capillary forces. Once the resin had contact with the hot stage, the selected cure cycle described in Section 2.2 was started. An optical microscope (Keyence VHX-2000) was used to make a 30 s interval time-lapse, allowing us to observe visual changes in the region of the epoxy/PEI interface.

2.4. Optical Interphase Analysis. Field emission scanning electron microscopy (JEOL JSM-7500F, Germany) and confocal laser scanning microscopy (Keyence 3D, VK-X1000) were used to study the interphase and morphology of cured samples. For CLSM, samples for analysis were embedded in a fast-cure epoxy resin and subsequently ground and polished. Polished samples were etched with *N*-methyl-2-pyrrolidone (NMP) following the procedure explained elsewhere[18] for qualitative observation of the interphase morphologies using the 20× objective of the CLSM. For SEM analysis, the etched samples were further coated with gold using a sputter coater.

2.5. Image Analysis. A time-resolved analysis was done on the images obtained during the hot-stage experiments. It is important to note that all the images, for a selected dwell time, were captured at the same position but at different time intervals (after every 30 s) during the curing process. To further quantify the movements of the epoxy front and PEI front, the ImageJ software[31] was used. The increment in diffusion lengths of epoxy and PEI fronts was measured by the difference between the position of the fronts at complete phase separation and the position of fronts at the beginning of second dwell.

To further analyze the interphase region and morphology, SEM microscopy was performed (Figure 3a). The micrographs were further

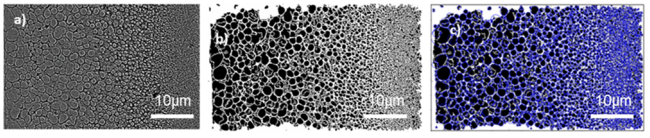

Figure 3. (a) SEM image of sample at 180 °C. (b) Segmented image from ImageJ. (c) Blob detection open CV.

examined to obtain the droplets' size and their distribution. A multi-stage thresholding and marker-based watershed image segmentation procedure was used to extract the droplets from the SEM images using Weka,[32] a machine learning segmentation tool in ImageJ (Figure 3b). The Python packages (Scikit-Image, SciPy, Numpy, and matplotlib) and blob detection with OpenCV[33] were used to calculate the droplet size across the interphase region (Figure 3c).

3. RESULTS

3.1. Interphase Formation. *3.1.1. Hot Stage.* Figure 4 shows the micrographs of a sample cured at 180 °C for two different first dwell times observed at different times in the two-dwell stage cycle. Figure 4a shows the existence of (i) a

https://doi.org/10.1021/acsapm.1c00956
ACS Appl. Polym. Mater. XXXX, XXX, XXX−XXX

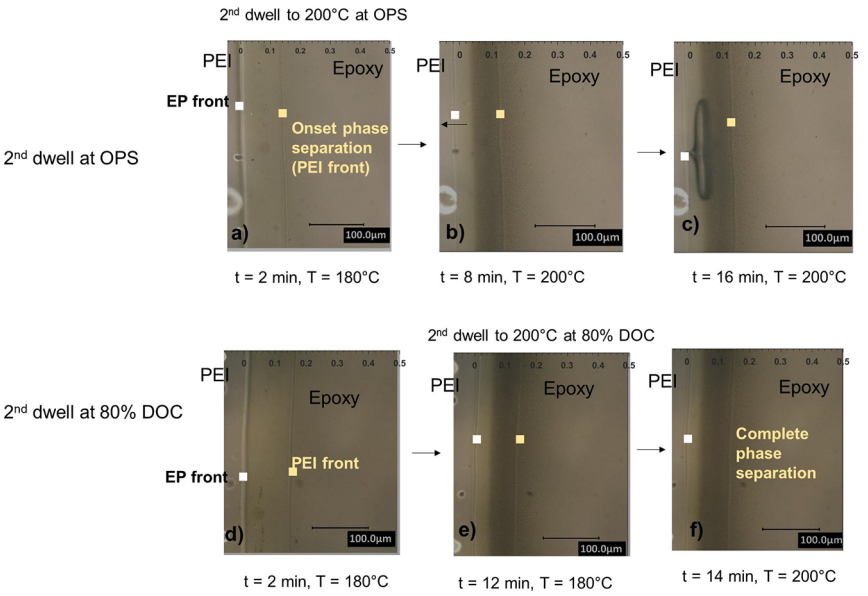

Figure 4. Optical micrographs of the sample at a 180 °C first dwell temperature. (a) Second dwell started just after the onset of phase separation (b, c) showing change in position of EP and PEI front through a pointer, (d) onset of phase separation, (e) second dwell started after 80% of degree of cure, and (f) complete phase separation after the second dwell. (OPS: onset of phase separation, DOC: degree of cure, the 0 mark on the horizontal axis indicates the initial interface between PEI and EP, and the upper scale bar is in millimeters).

penetration front of epoxy in the PEI film, (i.e., infiltration layer),[18] (ii) a darker region behind this epoxy front, which usually consisted of swollen thermoplastic resulting from the dissolution action of the epoxy monomers (i.e., gel layer),[18] and (iii) a clear interface between the gel layer and epoxy (PEI front), which indicated the onset of phase separation.[18]

Figure 4a–c presents the incremental evolution of the interphase region from the start of the second dwell (i.e., 200 °C) at the time of onset of phase separation (OPS case) during the first dwell. It is evident that both fronts (epoxy and PEI) progressed significantly overtime during the second dwell, even beyond the onset of phase separation. Figure 4d represents the onset of phase separation, while the second dwell started after achieving 80% degree of cure (80% DOC case) (Figure 4e–f): the progression of the diffusion front was small compared to the other case. To further quantify this movement, the distance traveled by the fronts during the second dwell is plotted as a function of the first dwell temperature for both cases in Figure 5. The results showed that the diffusion distance was significantly higher in the case of OPS as compared to the 80% DOC case, particularly at lower first dwell temperatures.

3.1.2. Interphase Analysis. The interphase formation between epoxy and PEI at different first dwell temperatures was analyzed by using SEM. The interphase regions of samples cured at 140 °C (first dwell temperature) for two different first dwell times (OPS and 80% DOC) are shown in Figure S3a,b, respectively. At this temperature, a distinct gradient morphology was clearly observed for both cases (OPS and 80% DOC). The SEM micrographs revealed the formation of a larger interphase region (71 μm) for the OPS case (Figure S3a) as compared to the 80% DOC case (56 μm) (Figure S3b). Similar results were also obtained for the samples pre-cured at 160 and 180 °C temperatures.

Figure 6 shows the interphase thickness as a function of first dwell temperature for both OPS and 80% DOC cases. It can be seen that the interphase thickness increased with the first dwell temperature for both cases, until 160 °C after which it slightly

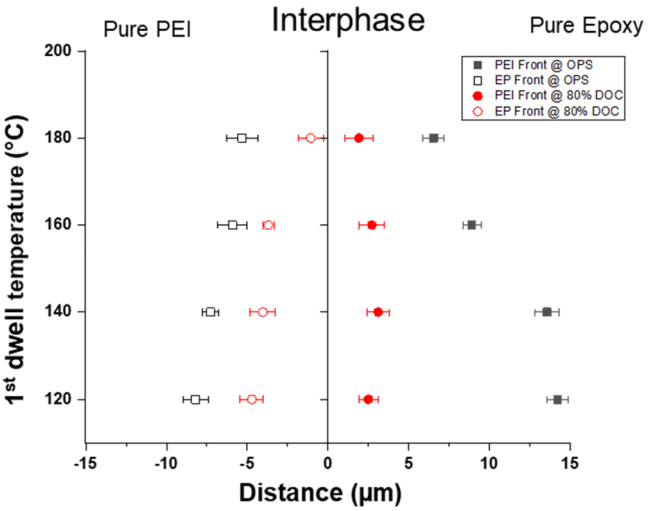

Figure 5. Increment in diffusion lengths of EP and PEI fronts as a function of temperature after onset of phase separation. Bars represent standard deviation.

decreased for a first dwell temperature of 180 °C. To better understand the effect of both first dwell cure temperature and time on the interphase formation, the relative difference in interphase thickness between the two cases (OPS and 80% DOC) is plotted as a function of first dwell temperature (Figure 7), with 80% DOC as a reference. The results displayed that the relative difference in interphase thickness was significantly higher at lower first dwell cure temperatures (i.e., ≤140 °C).

3.2. Morphological Analysis. The SEM images of a sample cured at 120 °C (1st dwell temperature) for the OPS case and 80% DOC case are presented in Figure S4a,b, respectively. The interphase formation was observed to be significantly different at a first dwell temperature of 120 °C, particularly for 80% DOC, as compared to higher first dwell temperatures. For instance, at a 120 °C first dwell temperature,

https://doi.org/10.1021/acsapm.1c00956
ACS Appl. Polym. Mater. XXXX, XXX, XXX−XXX

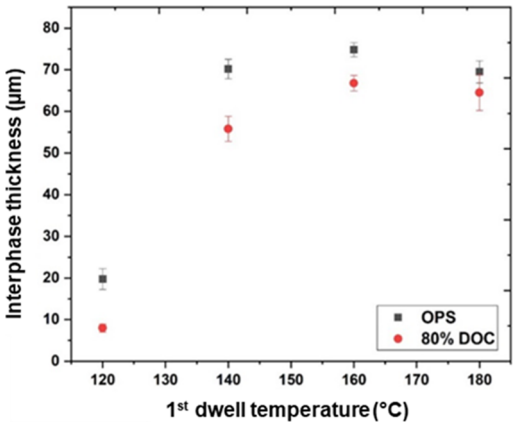

Figure 6. Final interphase thickness versus first dwell cure temperature at different first dwell times. (OPS: onset of phase separation, DOC: degree of cure).

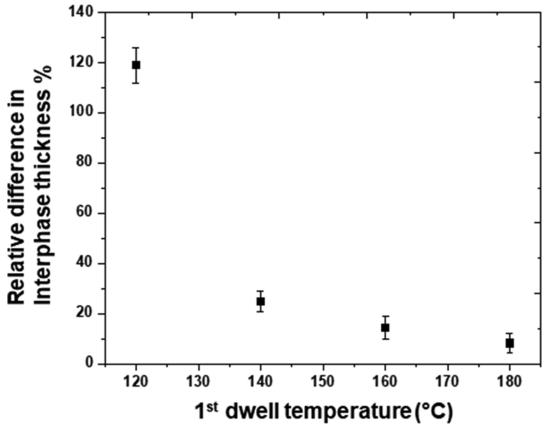

Figure 7. Relative difference in final interphase thickness between OPS and 80% DOC first dwell times as a function of first dwell temperature.

the formation of a gradient morphology was visible in the case of OPS (Figure S4a), while for 80% DOC (Figure S4b), no clear gradient morphology was evident at a much smaller interphase thickness. The SEM image of a sample cured at a 140 °C first dwell temperature until OPS, and then a second dwell at 200 °C is shown in Figure 8. The micrograph displays an epoxy/PEI biphasic region separated by a distinct interface of pure epoxy (left) and pure PEI (right). In the vicinity of the pure epoxy interface, the epoxy/PEI biphasic morphology was described by epoxy-rich droplets dispersed in a PEI matrix, i.e., phase-inverted morphology.[18] This phase inversion is attributed to the viscoelastic phase separation phenomenon, as already observed for different epoxy/thermoplastic blends.[34] The size of these epoxy droplets was observed to decrease gradually toward the pure PEI region due to the increase in PEI content. A similar gradient morphology was observed for the samples cured at higher dwell temperatures (160 and 180 °C).

3.3. Droplet Size Distribution. The epoxy droplet size and frequency, calculated from blob detection, are plotted as a function of position along the interphase for samples cured at different first dwell temperatures until OPS or 80% DOC (see Figure 9). It is evident from the graphs that the epoxy droplet size decreased by moving toward the pure PEI phase (i.e., from left to right) for all first dwell temperatures. Furthermore, the droplet size in the vicinity of the epoxy interface increased as a function of the first dwell cure temperature until 160 °C. Moreover, the frequency of smaller droplets was higher in the case of 80% DOC as compared to the OPS (see for instance Figure 9e,f). This behavior was also verified by the presence of the optically dense darker region in the CLSM image of a sample cured at a 140 °C first dwell temperature (80% DOC), as compared to the sample cured at a 140 °C first dwell temperature (OPS) (Figure 10). At a 120 °C first dwell temperature with 80% DOC (Figure 9b), a narrow droplet size distribution with an absence of smaller sizes was observed due to the absence of gradient morphology, as already discussed in Section 3.2 (see Figure S4b).

4. DISCUSSION

To understand the interphase formation in the EP/PEI system as a function of first dwell temperature and time, the degree of cure at the gel point (α_g) was estimated for the considered epoxy system using the Flory–Stockmayer relation, given as[35]

$$\alpha_g = \frac{1}{\sqrt{r(f_{w,e} - 1)(f_{w,a} - 1)}} \quad (1)$$

where, $f_{w,e}$ and $f_{w,a}$ are epoxy and amine average functionalities, respectively, while r represents the molar ratio of reacting functional groups and given as follows:

$$f_{w,e} = \frac{\sum f_e^2 N_e}{\sum f_e N_e} \quad (2)$$

$$f_{w,a} = \frac{\sum f_a^2 N_a}{\sum f_a N_a} \quad (3)$$

$$r = \frac{\sum f_e N_e}{\sum f_a N_a} \quad (4)$$

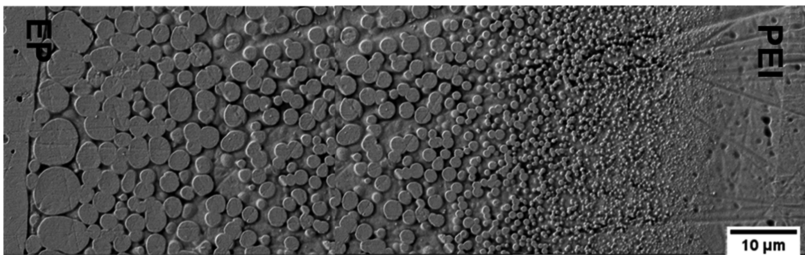

Figure 8. SEM micrograph showing phase-inverted morphology (epoxy-rich particles densely dispersed in a continuous PEI-rich matrix) of a PEI–epoxy interphase obtained at a 140 °C first dwell cure temperature (EP: epoxy).

https://doi.org/10.1021/acsapm.1c00956
ACS Appl. Polym. Mater. XXXX, XXX, XXX–XXX

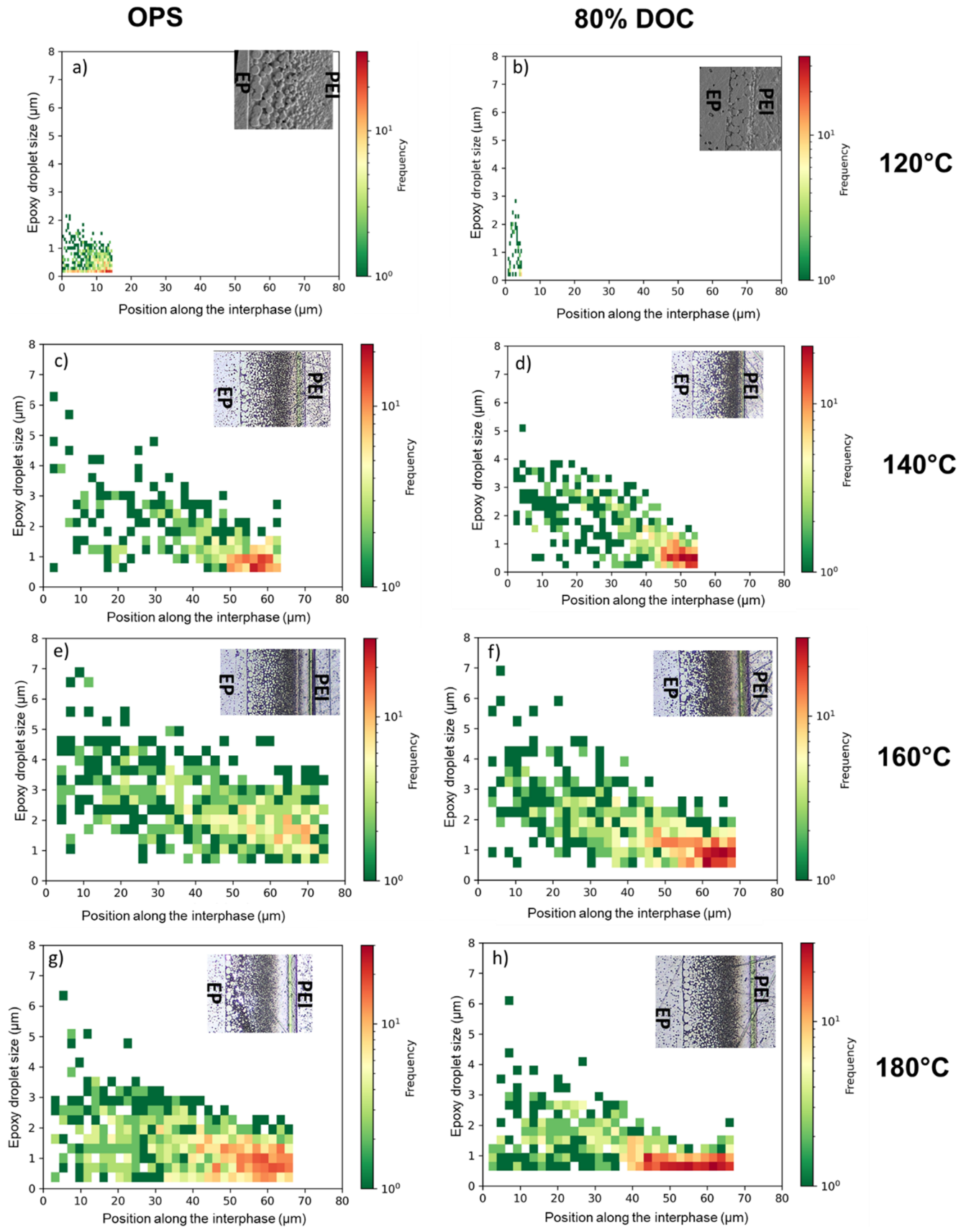

Figure 9. Epoxy droplet size from image analysis plotted as a function of position along the interphase (0 being pure EP) for samples (a), (c), (e), and (g) cured until OPS or (b), (d), (f), and (h) cured until 80% DOC at different first dwell temperatures (120−180 °C).

https://doi.org/10.1021/acsapm.1c00956
ACS Appl. Polym. Mater. XXXX, XXX, XXX−XXX

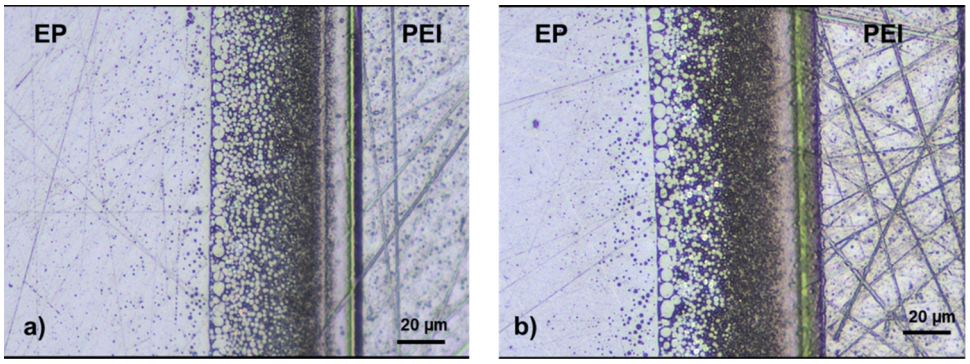

Figure 10. CLSM images showing interphase of a PEI/epoxy system obtained at 140 °C first dwell temperature; (a) second dwell at onset of phase separation and (b) second dwell at 80% degree of cure (EP: epoxy).

The functionalities of the epoxy monomers $f_{w,e}$ (DGEBF and TGMAP) were taken to be 2 and 3, respectively, while the functionality of DDS $f_{w,a}$ was 4.[36] N_e (0.03,0.14) and N_a (0.1) represent the number of moles of epoxy monomers (DGEBF and TGMAP) and amines (DDS), respectively. The estimated value of degree of cure at the gel point (α_g) was 0.43 for the considered epoxy system, which is in accordance with the literature value reported for a similar blend.[36] The degree of cure (estimated from the cure kinetics model, Figure 1b) as a function of first dwell temperature is plotted in Figure S5 for both OPS and 80% DOC cases. It is evident that for all OPS cases, the degree of cure was always lower than the one corresponding to the gel point (α_g), while the degree of cure was significantly higher than α_g for the 80% DOC case.

The outcome of hot-stage experiments, presented in Figure 4, showed higher diffusion distances in the OPS case as compared to the 80% DOC case, which may be attributed to the fact that the gel point was not attained in the OPS case, as shown in Figure S5, resulting in a higher diffusivity. This means that the epoxy polymeric chains/oligomers were still in a mobile state and can dissolve/diffuse further during the second dwell curing stage.[26] While at 80% DOC, the degree of cure was higher than the one corresponding to α_g, which theoretically means that the polymeric chains should be completely bound due to infinite molecular weight. However, a considerable diffusion distance was still observed at 80% DOC (Figure 5). This may be attributed to the demixing respectively non-stoichiometric curing, caused by the different diffusion speeds of three constituents of the epoxy system (TGMAP, DGEBF, and DDS). This effect became more pronounced for higher diffusion lengths (i.e., larger interphase) and higher temperatures. This means that at the diffusion front, the reaction rates derived from the bulk reaction kinetic model are optimistic. The slower reaction between epoxy monomers takes place, which eventually results in longer mobility and diffusion times even after achieving the nominal gel point. It is also interesting to note that the diffusion distance increased significantly by decreasing the first dwell temperature, particularly for the OPS case, which may be associated with the larger temperature difference between first dwell and second dwell conditions. This facilitated the diffusion/dissolution of polymeric chains.

Apart from analyzing the movement of diffusion fronts after the onset of phase separation using hot-stage microscopy, the SEM analysis provided a useful understanding of the morphology and total interphase thickness as a function of first dwell temperature and time. An increase in interphase thickness with increasing first dwell temperature (Figure 6) can be explained by the competition between the rate of phase separation and curing rate. If the phase separation proceeds much faster than the curing rate, then the interphase thickness is primarily controlled by the rate of phase separation rather than the cure rate (i.e., first dwell temperatures ≤ 160 °C). On the other hand, if the cure rate is faster than the phase separation, then the interphase thickness is controlled by the reaction rate (i.e., first dwell temperatures >160 °C).[18] A similar trend of increase in interphase thickness as a function of increasing first dwell temperature until 117 °C followed by a decrease in interphase thickness was observed for DGEBA epoxy toughened with polysiloxanes.[37] These authors attributed this increase/decrease in interphase thickness to the chemical reaction, coalescence, and interdiffusion of DGEBA and polysiloxanes. The thermoplastic (i.e., polysulfone) diffusion in the epoxy phase was also found to increase with the increase in the first dwell temperature, which was linked to the enhanced mobility of polymeric chains at higher temperatures.[26] Moreover, the relative difference in interphase thickness between OPS and 80% DOC (Figure 7) was quite significant particularly at lower first dwell temperatures, which again verifies the higher diffusion/dissolution of polymeric chains by starting second dwell at OPS for lower first dwell temperatures, as already discussed above. These results indicated that, apart from the first dwell temperature, the first dwell time (i.e., OPS and 80% DOC) influences the interphase thickness, particularly at lower first dwell temperatures.

In addition to interphase thickness, SEM analysis revealed a clear difference in interphase morphology as a function of first dwell temperature and time. The absence of a gradient morphology at a first dwell temperature of 120 °C (Figure S4) suggested the nonexistence of a concentration gradient, which supports the occurrence of case II diffusion for shorter lengths. While at higher first dwell temperatures, a clear concentration and morphology gradient became apparent (Figure 8), which may be attributed to the presence of a mixed mode between case I and case II diffusion. The formation of a similar gradient morphology was also observed in the literature for epoxy/PEI and PSU systems.[16]

In the end, the droplet size distribution in the interphase region was analyzed as a function of first dwell temperature and time. The size of bigger droplets in the vicinity of pure epoxy was observed to be significantly affected by the increase in the first dwell temperature until 160 °C (Figure 9), which may be attributed to the higher mobility of polymeric chains

https://doi.org/10.1021/acsapm.1c00956
ACS Appl. Polym. Mater. XXXX, XXX, XXX−XXX

before the onset of phase separation, favoring a longer growth phase after nucleation, as also observed in the literature.[38] However, the size of these bigger droplets was found to be independent of the first dwell time, as the onset of phase separation was achieved under similar conditions. Apart from bigger droplets, the frequency of smaller droplets was observed to be higher in the case of 80% DOC as compared to the OPS case, which may be linked to the restricted mobility of polymeric chains after phase separation, which eventually prevented the growth of particles and resulted in smaller droplets.[34] This hypothesis was further verified by the absence of these smaller droplets at 120 °C for the 80% DOC case.

5. CONCLUSIONS

The thermoplastic microphase is typically incorporated into the high T_g epoxy system to toughen the brittle epoxy by creating specific morphologies at the interphase. These morphologies and interphase dimensions can be fine-tuned by playing with the curing conditions of the modified epoxy system. Therefore, the main objective of the present study was to achieve the desired droplet size and interphase morphology for improved material toughness, which was attained by analyzing the influence of the dwell time and dwell temperature in the first dwell cycle. Hot-stage microscopy experiments were carried out at several first dwell temperatures in a range of 120−80 °C before final conversion at the second dwell. The morphologies and droplet size distribution at the interphase, after final cure, were further analyzed through scanning electron microscopy.

Hot-stage microscopy experiments revealed that both epoxy and PEI diffusion fronts continued to progress, even after achieving the onset of phase separation. However, the diffusion distance was significantly higher in the case of OPS as compared to the 80% DOC case, particularly at lower first dwell temperatures. SEM analysis showed that the interphase thickness was strongly influenced by both dwell temperature and dwell time. Furthermore, the size of bigger droplets near the pure epoxy region was primarily controlled by the dwell temperature, with almost no influence of dwell time. On the other hand, the frequency of smaller droplets was governed by dwell time. It is interesting to note that higher interphase thickness was obtained for the OPS case, while a larger number of smaller particles were observed for 80% DOC. Therefore, the influence of both these parameters (interphase thickness and droplets size) on the toughness enhancement of epoxy will be investigated in the future, along with the applications in the aerospace sector for producing fiber-reinforced epoxy composites. Moreover, in the case of 80% DOC, it will be interesting to analyze the sequential diffusion of monomer using the FTIR technique in order to explain the movement of epoxy and PEI diffusion fronts.

This work highlights the importance of the curing process beyond phase separation, using two-dwell cure cycles, to control the interphase dimension and final morphology for the poly(ether imide)/epoxy system.

ASSOCIATED CONTENT

Supporting Information

The Supporting Information is available free of charge at https://pubs.acs.org/doi/10.1021/acsapm.1c00956.

Representation of one-dwell cure cycle and two-dwell cure cycle; SEM micrograph showing phase-inverted morphology (epoxy-rich particles densely dispersed in a continuous PEI-rich matrix) of a PEI−epoxy interphase obtained at a 180 °C cure temperature; selected first dwell temperature and time; SEM micrograph showing the interphase of a PEI/epoxy system obtained at a 140 °C first dwell temperature; SEM micrograph showing the interphase of a PEI/epoxy system obtained at a 120 °C first dwell temperature; second dwell at onset of phase separation and second dwell at 80% degree of cure (EP: epoxy); and degree of cure reached at the end of fist dwell temperature for both cases, OPS, and 80% DOC (PDF)

AUTHOR INFORMATION

Corresponding Author

Ujala Farooq − *Faculty of Aerospace Engineering, Aerospace Manufacturing Technologies, Delft University of Technology, 2629 HS Delft, the Netherlands;* orcid.org/0000-0002-6001-3765; Email: U.Farooq@tudelft.nl

Authors

Sönke Heuer − *Technische Universität Braunschweig, Institut für Adaptronik und Funktionsintegration (IAF), 38106 Braunschweig, Germany*

Julie Teuwen − *Faculty of Aerospace Engineering, Aerospace Manufacturing Technologies, Delft University of Technology, 2629 HS Delft, the Netherlands*

Clemens Dransfeld − *Faculty of Aerospace Engineering, Aerospace Manufacturing Technologies, Delft University of Technology, 2629 HS Delft, the Netherlands*

Complete contact information is available at: https://pubs.acs.org/10.1021/acsapm.1c00956

Notes

The authors declare no competing financial interest.

ACKNOWLEDGMENTS

The authors acknowledge Petra Inderkum, Ekaterina Sakarinen, and Julien Asquier for further developing the methodology. They would also like to thank Prof. Christian Brauner from the Institute of Polymer Engineering, FHNW, Switzerland, Kunal Masania from TU Delft, and Petra Inderkum from Complex Materials, ETH Zurich, Switzerland for fruitful discussions.

REFERENCES

(1) Pulikkalparambil, H.; Rangappa, S.M.; Siengchin, S.; Parameswaranpillai, J. Introduction to Epoxy Composites. In *Epoxy Composites*; Wiley-VCH: 2021, DOI: 10.1002/9783527824083.ch1pp. 1−21.

(2) Kim, J.; Baillie, C.; Poh, J.; Mai, Y.-W. Fracture toughness of CFRP with modified epoxy resin matrices. *Compos. Sci. Technol.* **1992**, *43*, 283−297.

(3) Shi, X.-H.; Xu, Y.-J.; Long, J.-W.; Zhao, Q.; Ding, X.-M.; Chen, L.; Wang, Y.-Z. Layer-by-layer assembled flame-retardant architecture toward high-performance carbon fiber composite. *Chem. Eng. J.* **2018**, *353*, 550−558.

(4) Qiu, Y.; Qian, L.; Feng, H.; Jin, S.; Hao, J. Toughening effect and flame-retardant behaviors of phosphaphenanthrene/phenylsiloxane bigroup macromolecules in epoxy thermoset. *Macromolecules* **2018**, *51*, 9992−10002.

(5) Pruksawan, S.; Samitsu, S.; Yokoyama, H.; Naito, M. Homogeneously dispersed polyrotaxane in epoxy adhesive and its

improvement in the fracture toughness. *Macromolecules* **2019**, *52*, 2464−2475.
(6) Deng, S.; Djukic, L.; Paton, R.; Ye, L. Thermoplastic−epoxy interactions and their potential applications in joining composite structures−A review. *Composites Part A: Applied Science and Manufacturing* **2015**, *68*, 121−132.
(7) Hamerton, I.; McNamara, L. T.; Howlin, B. J.; Smith, P. A.; Cross, P.; Ward, S. Toughening mechanisms in aromatic polybenzoxazines using thermoplastic oligomers and telechelics. *Macromolecules* **2014**, *47*, 1946−1958.
(8) Jayan, J. S.; Saritha, A.; Joseph, K. Innovative materials of this era for toughening the epoxy matrix: A review. *Polym. Compos.* **2018**, *39*, E1959−E1986.
(9) Unnikrishnan, K. P.; Thachil, E. T. Toughening of epoxy resins. *Des. Monomers Polym.* **2006**, *9*, 129−152.
(10) Parameswaranpillai, J.; Krishnan Sidhardhan, S.; Jose, S.; Siengchin, S.; Pionteck, J.; Magueresse, A.; Grohens, Y.; Hameed, N. Reaction-induced phase separation and resulting thermomechanical and surface properties of epoxy resin/poly(ethylene oxide)−poly(propylene oxide)−poly(ethylene oxide) blends cured with 4,4′-diaminodiphenylsulfone. *J. Appl. Polym. Sci.* **2017**, *134*, DOI: 10.1002/app.44406.
(11) Farooq, U.; Teuwen, J.; Dransfeld, C. Toughening of Epoxy Systems with Interpenetrating Polymer Network (IPN): A Review. *Polymer* **2020**, *12*, 1908.
(12) Hubert, P.; Centea, T.; Grunefelder, L.; Nutt, S.; Kratz, J.; Lévy, A. Out-of-Autoclave Prepreg Processing. In *Comprehensive Composite Materials II*, Elsevier: 2018; pp. 63−94.
(13) Ramsdale-Capper, R.; Foreman, J. P. Internal antiplasticisation in highly crosslinked amine cured multifunctional epoxy resins. *Polymer* **2018**, *146*, 321−330.
(14) Swier, S.; Van Mele, B. Mechanistic Modeling of the Epoxy−Amine Reaction in the Presence of Polymeric Modifiers by Means of Modulated Temperature DSC. *Macromolecules* **2003**, *36*, 4424−4435.
(15) Ekbrant, B.r. E. F.; Skov, A. L.; Daugaard, A. E. Epoxy-Rich Systems with Preference for Etherification over Amine-Epoxy Reactions for Tertiary Amine Accelerators. *Macromolecules* **2021**, 4280−4287.
(16) Vandi, L.-J.; Hou, M.; Veidt, M.; Truss, R.; Heitzmann, M.; Paton, R. Interface diffusion and morphology of aerospace grade epoxy co-cured with thermoplastic polymers. In *Proceedings of 28th International Congress of the Aeronautical Sciences (ICAS 2012)*.
(17) Lestriez, B.; Chapel, J.-P.; Gérard, J.-F. Gradient interphase between reactive epoxy and glassy thermoplastic from dissolution process, reaction kinetics, and phase separation thermodynamics. *Macromolecules* **2001**, *34*, 1204−1213.
(18) Teuwen, J. J. E.; Asquier, J.; Inderkum, P.; Masania, K.; Brauner, C.; Villegas, I. F.; Dransfeld, C. Gradient interphases between high T g epoxy and polyetherimide for advanced joining processes. *Proceedings of the ECCM18, Athens, Greece* **2018**, 24−28.
(19) Rico, M.; López, J.; Montero, B.; Bellas, R. Phase separation and morphology development in a thermoplastic-modified toughened epoxy. *Eur. Polym. J.* **2012**, *48*, 1660−1673.
(20) Yu, Y.; Shen, G.; Liu, Z. Morphology of Epoxy/Thermoplastic Blends. In *Handbook of Epoxy Blends*, Parameswaranpillai, J.; Hameed, N.; Pionteck, J.; Woo, E.M., Eds. Springer International Publishing: Cham, 2015; DOI: 10.1007/978-3-319-18158-5_18-1 pp. 1−34.
(21) Tercjak, A. Phase separation and morphology development in thermoplastic-modified thermosets. In *Thermosets*, Elsevier: 2018; pp. 147−171.
(22) Harismendy, I.; Del Rio, M.; Marieta, C.; Gavalda, J.; Mondragon, I. Dicyanate ester−polyetherimide semi-interpenetrating polymer networks. II. Effects of morphology on the fracture toughness and mechanical properties. *J. Appl. Polym. Sci.* **2001**, *80*, 2759−2767.
(23) Mimura, K.; Ito, H.; Fujioka, H. Improvement of thermal and mechanical properties by control of morphologies in PES-modified epoxy resins. *Polymer* **2000**, *41*, 4451−4459.
(24) Cho, J. B.; Hwang, J. W.; Cho, K.; An, J. H.; Park, C. E. Effects of morphology on toughening of tetrafunctional epoxy resins with poly (ether imide). *Polymer* **1993**, *34*, 4832−4836.
(25) Harismendy, I.; Del Rio, M.; Eceiza, A.; Gavalda, J.; Gomez, C.; Mondragon, I. Morphology and thermal behavior of dicyanate ester-polyetherimide semi-IPNS cured at different conditions. *J. Appl. Polym. Sci.* **2000**, *76*, 1037−1047.
(26) Bian, D.; Beeksma, B. R.; Shim, D. J.; Jones, M.; Lawrence Yao, Y. Interlaminar toughening of GFRP—part i: Bonding improvement through diffusion and precipitation. *Journal of Manufacturing Science and Engineering* **2017**, *139*, No. 071010.
(27) Kim, Y.-S.; Min, H.-S.; Kim, S.-C. Polyetherimide/dicyanate semi-interpenetrating polymer networks having a morphology spectrum. *Macromol. Res.* **2002**, *10*, 60−66.
(28) Villegas, I. F.; van Moorleghem, R. Ultrasonic welding of carbon/epoxy and carbon/PEEK composites through a PEI thermoplastic coupling layer. *Composites Part A: Applied Science and Manufacturing* **2018**, *109*, 75−83.
(29) Heitzmann, M.T.; Hou, M.; Veidt, M.; Vandi, L.J.; Paton, R. Morphology of an interface between polyetherimide and epoxy prepreg. In *Proceedings of Advanced Materials Research*; pp. 184−188.
(30) Voleppe, Q.; Pardoen, T.; Bailly, C. Interdiffusion and phase separation upon curing in thermoset-thermoplastic interphases unravelled by the characterization of partially cured systems. *Polymer* **2016**, *106*, 120−127.
(31) Schneider, C. A.; Rasband, W. S.; Eliceiri, K. W. NIH Image to ImageJ: 25 years of image analysis. *Nat. Methods* **2012**, *9*, 671−675.
(32) Eibe, F.; Hall, M. A.; Witten, I. H.; Pal, J. The WEKA workbench. *Online appendix for data mining: practical machine learning tools and techniques* **2016**, *4*, 28.
(33) Bradski, G. The opencv library. *Dr Dobb's J. Software Tools* **2000**, *25*, 120−125.
(34) Surendran, A.; Joy, J.; Parameswaranpillai, J.; Anas, S.; Thomas, S. An overview of viscoelastic phase separation in epoxy based blends. *Soft Matter* **2020**, *16*, 3363−3377.
(35) Hammond, P. *Synthesis of Polymers MIT OpenCourseWare: Massachusetts Institute of Technology*, 2006.
(36) Rosetti, Y.; Alcouffe, P.; Pascault, J.-P.; Gérard, J.-F.; Lortie, F. Polyether sulfone-based epoxy toughening: from micro-to nano-phase separation via PES end-chain modification and process engineering. *Materials* **2018**, *11*, 1960.
(37) Cabanelas, J. C.; Serrano, B.; Gonzalez, M. G.; Baselga, J. Confocal microscopy study of phase morphology evolution in epoxy/polysiloxane thermosets. *Polymer* **2005**, *46*, 6633−6639.
(38) Ma, H.; Aravand, M. A.; Falzon, B. G. Phase morphology and mechanical properties of polyetherimide modified epoxy resins: a comparative study. *Polymer* **2019**, *179*, 121640.

https://doi.org/10.1021/acsapm.1c00956
ACS Appl. Polym. Mater. XXXX, XXX, XXX−XXX